Mass-Spectrometric Experiments together with Electronic Structure Calculations Support the Existence of the Elusive Ammonia Oxide Molecule and Its Radical Cation☆

Mark Brönstrup, Detlef Schröder, Ilona Kretzschmar, Christoph A. Schalley[+], and Helmut Schwarz*

Institut für Organische Chemie der Technischen Universität Berlin,
Straße des 17. Juni 135, D-10623 Berlin
Fax: (internat.) + 49(0)30/314-21102
E-mail: schw0531@www.chm.tu-berlin.de

Received May 12, 1998

Keywords: Ab initio calculations / Mass spectrometry / Gas-phase chemistry / Ammonia oxide / Hydroxylamine

Mass-spectrometric experiments were combined with ab initio calculations to explore the cationic and neutral $[H_3,N,O]^{\bullet+/0}$ potential energy surfaces and relevant anionic species. The calculations predict the existence of three stable cationic and neutral $[H_3,N,O]^{\bullet+/0}$ isomers, i.e. ammonia oxide $H_3NO^{\bullet+/0}$ (**1**$^{\bullet+/0}$), hydroxylamine $H_2NOH^{\bullet+/0}$ (**2**$^{\bullet+/0}$) and the imine-water complex $HNOH_2^{\bullet+/0}$ (**3**$^{\bullet+/0}$). Hydroxylamine **2** represents the most stable isomer on the neutral surface (E_{rel} = 0), and the metastable isomers **1** (E_{rel} = 24.8 kcal mol^{-1}) and **3** (E_{rel} = 61.4 kcal mol^{-1}) are separated by barriers of 49.5 kcal mol^{-1} and 64.2 kcal mol^{-1}, respectively. Adiabatic ionization of **2** (IE_a = 9.15 eV) yields **2**$^{\bullet+}$, which is 21.4 kcal mol^{-1} more stable than **1**$^{\bullet+}$ and 36.4 kcal mol^{-1} more stable than **3**$^{\bullet+}$. The barriers associated with the isomerizations of the cations are 58.6 kcal mol^{-1} for **2**$^{\bullet+}$ → **1**$^{\bullet+}$ and 71.4 kcal mol^{-1} for **2**$^{\bullet+}$ → **3**$^{\bullet+}$. Collisional activation (CA) and unimolecular decomposition (MI) experiments allow for a clear distinction of **1**$^{\bullet+}$ from **2**$^{\bullet+}$. Besides, neutralization/reionization (NR) experiments strongly support the gas-phase existence of the long-sought neutral ammonia oxide.

Introduction

The generation of ammonia oxide (**1**) represents a major challenge to experimentalists working in the field of elusive molecules, as there is a striking discrepancy between the numerous quantum chemical studies,[1] which predict a distinct stability of the molecule, and the still scarce experimental evidence.[2] Moreover, it has recently been stated that "the *possible* characterization of two metastable isomers of hydroxylamine ... would be a significant step forward towards the understanding of important aspects of N/O/H chemistry."[2a]

The fact that homologs of **1** like trialkylamine oxides are well-known, storable compounds indicates that the atom connectivity R_3N-O is not inherently unstable. Therefore, for R = H the main problem is to prevent the isomerization of **1** to the more stable hydroxylamine (**2**). This can occur in two ways, i.e. either a unimolecular [1,2]-H shift or a bi- or termolecular acid/base-catalyzed path, of which we presume the latter to be energetically favorable. Such an acid/base-catalyzed isomerization can be circumvented by generating the species of interest in the diluted gas phase of a mass spectrometer. The generation and characterization of several elusive ionic and neutral molecules has been achieved during the last decade by combining advanced mass-spectrometric techniques, like collisional activation (CA) and neutralization/reionization (NR), with appropriate theoretical means.[3][4]

Nowadays, theoretical calculations of small systems, like $[H_3,N,O]$, can achieve an accuracy such that they do complement the experimental results. Therefore, we have performed a series of mass-spectrometric experiments and calculated all relevant structures of the cationic and neutral $[H_3,N,O]$ surfaces with a G2-like ab initio method; also the anionic species are briefly discussed (see below). The neutral surface was reexamined using the same level of theory, as previous theoretical studies did not include the relevant exit channels. For the sake of simplicity and readability, the potential energy surfaces (PES) of the different charge states are calibrated to the respective global minima, which are set to zero (E_{rel} = 0). As all the experiments start from cationic states, the cationic PES will be discussed first.

Theoretical Results

The relative energies of all relevant species of the $[H_3,N,O]^{\bullet+}$ surface are displayed in Table 1. Ionized hydroxylamine (**2**$^{\bullet+}$) represents the global minimum (E_{rel} = 0) and possesses a planar structure. Mulliken analysis reveals that the spin density is distributed between the nitrogen (0.80) and the oxygen atom (0.20). This indicates that the unpaired electron is mainly located on the nitrogen atom, but that there is also exchange with the adjacent oxygen lone pairs. As a consequence, the N−O bond length is significantly shortened compared to neutral hydroxylamine (128 pm vs. 144 pm, see below). A [1,2]-H shift from the nitrogen to the oxygen atom requires an energy of 58.6 kcal mol^{-1} and leads to the ammonia oxide cation (**1**$^{\bullet+}$), which

[+] Present address: The Skaggs Institute for Chemical Biology, The Scripps Research Institute, 10550 North Torrey Pines Road, La Jolla, CA, 92037, USA.

 © WILEY-VCH Verlag GmbH, D-69451 Weinheim, 1998 1434−1948/98/1010−1529 $ 17.50+.50/0

is a minimum with E_{rel} = 21.4 kcal mol^{-1}. Thus, the calculations suggest that the ammonia oxide cation (**1**$^{\bullet+}$) is trapped in a potential well which may be deep enough to capture **1**$^{\bullet+}$ without facile isomerization to **2**$^{\bullet+}$ or dissociation. With respect to the lowest lying direct exit channel for the dissociation of $[H_3,N,O]^{\bullet+}$, i.e. loss of H$^\bullet$ (E_{rel} = 69.7 kcal mol^{-1}), unimolecular isomerization **1**$^{\bullet+}$ ⇌ **2**$^{\bullet+}$ is, however, conceivable. The ammonia oxide cation (**1**$^{\bullet+}$) has C_s symmetry due to a small Jahn-Teller distortion of the C_{3v}-symmetric molecule. The unpaired electron is located on the oxygen atom (spin density = 1.05). In contrast to hydroxylamine, the N−O bond is not shortened, but slightly elongated upon ionization of the neutral **1** (138 pm vs. 135 pm, see below); this can be explained in terms of a diminished electrostatic interaction compared to the neutral $H_3N^+-O^-$ zwitterion. Another minimum structure of $[H_3,N,O]^{\bullet+}$ is obtained by a [1,2]-H shift from the nitrogen to the oxygen atom starting from hydroxylamine. The resulting distonic ion **3**$^{\bullet+}$ (E_{rel} = 36.4 kcal mol^{-1}) can be regarded as an ion-dipole complex between the imine fragment (*IE* = 13.49 eV) and the water cation (*IE* = 12.612 eV).[5] The barrier associated with this [1,2]-H shift (E_{rel} = 71.4 kcal mol^{-1}) implies that the $NH_2OH^{\bullet+}/NHOH_2^{\bullet+}$ isomerization is disfavored compared to the $NH_2OH^{\bullet+}/NH_3O^{\bullet+}$ equilibrium. Moreover, the exit channel for loss of H$^\bullet$ to yield H_2NO^+ **4**$^+$ is lower in energy (E_{rel} = 69.7 kcal mol^{-1}) and has much smaller entropical restrictions than the rearrangement **2**$^{\bullet+}$ → **3**$^{\bullet+}$. Therefore, we expect that $NHOH_2^{\bullet+}$ (**3**$^{\bullet+}$), can hardly be generated by isomerization starting from **1**$^{\bullet+}$ and **2**$^{\bullet+}$ when the $[H_3,N,O]^{\bullet+}$ surface is accessed experimentally. A further proton shift from the nitrogen to the oxygen atom and consecutive fragmentation yields H_3O^+ and N (^4S) as the lowest lying exit channel of the cationic PES (E_{rel} = 49.3 kcal mol^{-1}). However, as H_3O^+ and N (^4S) can only be produced after spin crossing and extensive isomerization, severe kinetic restrictions are imposed on this otherwise thermochemically favorable exit channel.

Cleavage of one of the N−H bonds in ionized hydroxylamine (**2**$^{\bullet+}$) gives H$^\bullet$ and *cis*- or *trans*-$HNOH^+$ (**5**$^+$) with E_{rel} = 87.0 kcal mol^{-1} (*trans*) and 93.6 kcal mol^{-1} (*cis*), respectively (Table 2).[6] Further exit channels of $[H_3,N,O]^{\bullet+}$ yield $HNO^{\bullet+}$ (**6**$^{\bullet+}$) and H_2 (E_{rel} = 58.4 kcal mol^{-1}), $NOH^{\bullet+}$ (**7**$^{\bullet+}$) and H_2 (E_{rel} = 73.2 kcal mol^{-1}), or NO^+, **8**$^+$, H_2, and H$^\bullet$ (E_{rel} = 77 kcal mol^{-1}). Although these exit channels are low in energy, they are associated with significant activation barriers. Thus, the transition state **TS 1**$^{\bullet+}$**/6**$^{\bullet+}$ for 1,1-elimination of H_2 from **1**$^{\bullet+}$ has a relative energy of 89.5 kcal mol^{-1}, and the transition state **TS 2**$^{\bullet+}$**/7**$^{\bullet+}$ for the analogous 1,1-elimination of H_2 from **2**$^{\bullet+}$ has a relative energy of 92.3 kcal mol^{-1}. Despite an intensive search from several starting geometries, a transition state for a formal 1,2-elimination from **2**$^{\bullet+}$ could not be located. Instead, optimization leads to two transition structures **TS 5**$^+$**/6**$^{\bullet+}$ and **TS 4**$^+$**/6**$^{\bullet+}$, which are featured by linear O−H−H (**TS 5**$^+$**/6**$^{\bullet+}$) and N−H−H (**TS 4**$^+$**/6**$^{\bullet+}$) arrangements. An analysis of the internal reaction coordinate (IRC) reveals that the respective reaction pathways correspond to an attack of a hydrogen atom at H_2NO^+ (**4**$^+$) and at $HNOH^+$ (**5**$^+$), respectively, to yield $HNO^{\bullet+}$ (**6**$^{\bullet+}$) and H_2. Although the barriers associated with these transition structures are comparable to those for **TS 1**$^{\bullet+}$**/6**$^{\bullet+}$ and **TS 2**$^{\bullet+}$**/7**$^{\bullet+}$, it is hard to imagine that **TS 4**$^+$**/6**$^{\bullet+}$ or **TS 5**$^+$**/6**$^{\bullet+}$ can be reached, because instead of a long-range H migration starting from **1**$^{\bullet+}$ or **2**$^{\bullet+}$, an irreversible loss of the migrating hydrogen atom appears to be favored. Therefore, it is suggested that the only ways to produce $HNO^{\bullet+}/H_2$ from $[H_3,N,O]^{\bullet+}$ proceed by 1,1-eliminations (**TS 1**$^{\bullet+}$**/6**$^{\bullet+}$ and **TS 2**$^{\bullet+}$**/7**$^{\bullet+}$). Two different pathways of NO^+ generation from $[H_3,N,O]^{\bullet+}$ are conceivable: Either H_2 elimination to yield $[H,N,O]^{\bullet+}$ precedes H$^\bullet$ abstraction, or H$^\bullet$ is lost first to yield **4**$^+$ and/or **5**$^+$, which can subsequently be dehydrogenated to NO^+. The calculations predict that the initial H_2 eliminations either from **1**$^{\bullet+}$ or from **2**$^{\bullet+}$ are strongly favored by at least 66.1 kcal mol^{-1} compared to the dehydrogenations of **4**$^+$ and **5**$^+$ (Figure 1). Therefore, it can be concluded that only the pathway involving loss of H_2 followed by loss of H$^\bullet$ is relevant for NO^+ production in the present context.

Losses of one or several hydrogen atoms do not reveal information about the connectivity of the $[H_3,N,O]^{\bullet+}$ precursors. For a structural elucidation, fragments arising from cleavage of the N−O bond are decisive: Cleavage of N−O in **2**$^{\bullet+}$ into NH_2^+ ($^3B_1$) and OH$^\bullet$ has an energy demand of E_{rel} = 104.0 kcal mol^{-1}, whereas the N−O cleavage of **1**$^{\bullet+}$ to yield O (^3P) and $NH_3^{\bullet+}$ requires E_{rel} = 79.4 kcal mol^{-1}. For **2**$^{\bullet+}$, the calculations predict a competition of two processes: The direct bond cleavage into NH_2^+ ($^3B_1$) and OH$^\bullet$ is energetically disfavored, but has probably no kinetic restriction. In contrast, while the production of $NH_3^{\bullet+}$ + O

Table 1. Total energies *E* in Hartree for $[H_3, N, O]^{\bullet+/0}$ species; *E* = *E*[CCSD(T)/6-311G(d,p)] + *E*[MP2/6-311+G(3df,2p)] − *E*[MP2/6-311G(d,p)] + ZPVE

Species	Total energy in Hartree
NH_3O (**1**)	−131.453218
$^3NH_3O$ (^{3}**1**)	−131.403453
NH_3O, with geometry of **1**$^{\bullet+}$	−131.451865
NH_2OH (**2**)	−131.492710
$^3NH_2OH$ (^{3}**2**)	−131.399248
NH_2OH, gauche,gauche conf.	−131.486162
NH_2OH, with geometry of **2**$^{\bullet+}$	−131.444508
$NHOH_2$ (**3**)	−131.394834
MECP $^1NH_3O/^3NH_3O$	−131.387307
TS 1/2	−131.413806
TS 2/3	−131.390428
TS 2/6	−131.314067
TS 2/7	−131.351575
TS 1/6	−131.375234
$NH_3O^{\bullet+}$ (**1**$^{\bullet+}$)	−131.119145
$NH_3O^{\bullet+}$, with geometry of **1**	−131.118677
$NH_2OH^{\bullet+}$ (**2**$^{\bullet+}$)	−131.156460
$NH_2OH^{\bullet+}$, with geometry of **2**	−131.098877
$NHH_2O^{\bullet+}$ (**3**$^{\bullet+}$)	−131.098450
TS 1$^{\bullet+}$**/2**$^{\bullet+}$	−131.063322
TS 2$^{\bullet+}$**/6**$^{\bullet+}$	−131.001773
TS 1$^{\bullet+}$**/6**$^{\bullet+}$	−131.013807
TS 2$^{\bullet+}$**/6**$^{\bullet+}$	−131.042749
TS 2$^{\bullet+}$**/7**$^{\bullet+}$	−131.009346
TS 5$^+$**/6**$^{\bullet+}$	−131.001773
TS 4$^+$**/6**$^{\bullet+}$	−131.015157

Table 2. Total energies E in Hartree for $[H_3,N,O]^{\bullet+/0}$ fragmentation products; $E = E$[CCSD(T)/6-311G(d,p)) + E(MP2/6-311+G-(3df,2p)] − E[MP2/6-311G(d,p)] + ZPVE

Species	Total energy in Hartree
$H_2NO^\bullet$ (**4**$^\bullet$)	−130.871158
trans-$HNOH^\bullet$ (**5**$^\bullet$)	−130.860474
cis-$HNOH^\bullet$ (**5**$^\bullet$)	−130.852498
HNO (**6**)	−130.282162
^3NOH (**7**)	−130.237766
$NO^\bullet$ (**8**$^\bullet$)	−129.701610
NH_3	−56.435131
^3O	−74.966971
$OH^\bullet$	−75.625497
$H_2N^\bullet$	−55.770735
H_2	−1.160442
H	−0.499810
^4N	−54.510044
^3NH	−55.126862
^1NH	−55.060045
H_2O	−76.308577
NH_2O^+ (**4**$^+$)	−130.545642
trans-$NHOH^+$ (**5**$^+$)	−130.517986
cis-$NHOH^+$ (**5**$^+$)	−130.507510
$NHO^{\bullet+}$ (**6**$^{\bullet+}$)	−129.902885
$NOH^{\bullet+}$ (**7**$^{\bullet+}$)	−129.879370
NO^+ (**8**$^+$)	−129.373546
TS 4$^+$**/8**$^+$	−130.404296
TS 5$^+$**/8**$^+$	−130.383696
$NH_3^{\bullet+}$	−56.062959
$^1NH_2^+$	−55.316852
$^3NH_2^+$	−55.365182
$H_2O^{\bullet+}$	−75.847343
$NH^{\bullet+}$	−54.636206
H_3O^+	−76.56788

and $NH_3^{\bullet+}$ is favored due to thermochemical *and* kinetic reasons.

The profile of the neutral $[H_3,N,O]$ surface resembles its cationic counterpart as far as the hydroxylamine/ammonia oxide region is concerned. Hydroxylamine (**2**) again represents the global minimum and has two C_s-symmetrical conformers which differ in energy by 4.1 kcal mol^{-1} (E_{rel} = 0 for θ_{HNOH} = 125.1°, E_{rel} = 4.1 kcal mol^{-1} for θ_{HNOH} = 57.4°). Hydroxylamine (**2**) can isomerize to ammonia oxide (**1**) by a [1,2]-H shift with an energy barrier of 49.5 kcal mol^{-1}. **1** lies 24.8 kcal mol^{-1} higher in energy than **2**, but may be captured as a metastable molecule due to the reverse barrier of 24.7 kcal mol^{-1} towards isomerization to **2** and a barrier of 48.9 kcal mol^{-1} associated with fragmentation into HNO and H_2. The N−O bond in **1** is significantly shorter than in **2** (135 pm vs. 144 pm), which can be rationalized with an electrostatic attraction of the zwitterionic **1** and the repulsion of lone pairs in **2**. The two molecules are predicted to differ also in other physical properties such as dipole moments[7] (μ = 5.63 D for **1** and 0.788 D for **2**) or vertical ionization energies[8][9] (IE_v = 9.1 eV for **1** and 10.72 eV for **2**). Two factors are mainly responsible for the fact that vertically ionized hydroxylamine is 36.1 kcal mol^{-1} above the minimum geometry of the cation. First, the minimum-energy conformation of **2**$^{\bullet+}$ is planar, while C_s-symmetrical, neutral **2** has a dihedral HNOH angle of 125°. Secondly, the N−O bond lengths in **2** and **2**$^{\bullet+}$ differ significantly (Figures 3 and 4). In contrast, the geometry changes upon adiabatic ionization of **1** are negligible, and IE_a and

Figure 1. Potential energy surface of cationic $[H_3,N,O]^{\bullet+}$; zero-point corrected energies given in kcal mol^{-1} relative to $H_2NOH^{\bullet+}$ (**2**$^{\bullet+}$)

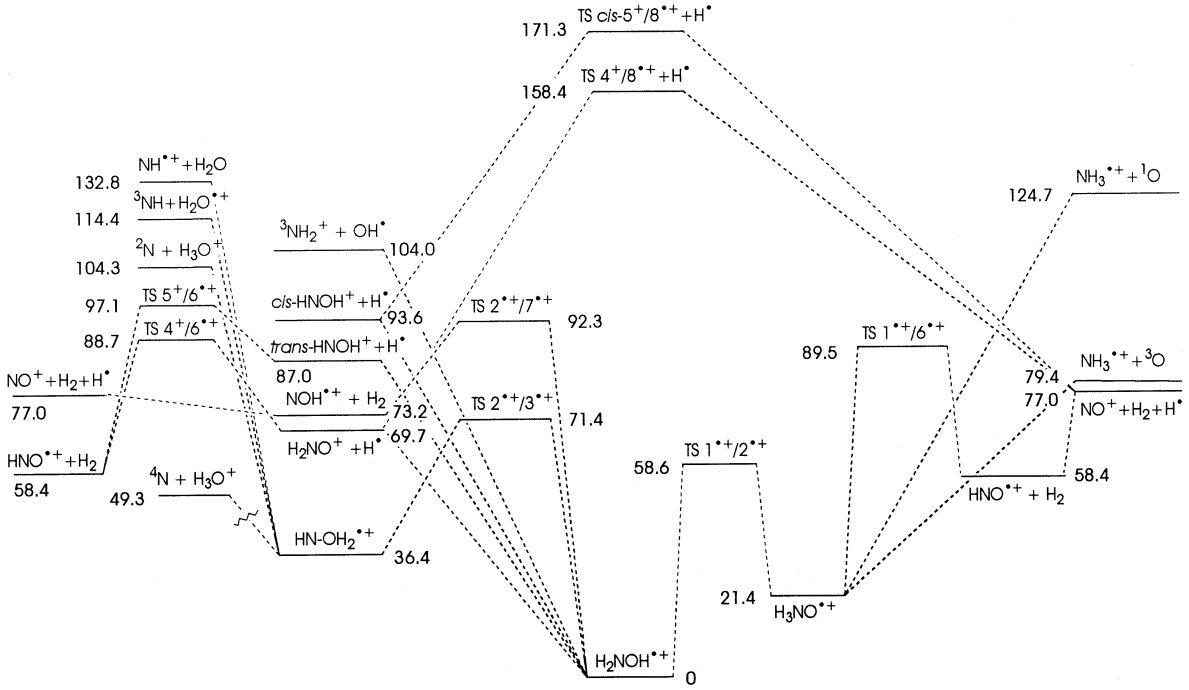

is lower in energy, it is kinetically hampered due to the entropic restrictions associated with **TS 1**$^{\bullet+}$**/2**$^{\bullet+}$. For ionized ammonia oxide, however, the direct fragmentation into O

IE_v differ by no more than 0.29 kcal mol^{-1}. As a result, the vertical ionization energies of hydroxylamine (IE_v = 10.72 eV) and ammonia oxide (IE_v = 9.1 eV) differ by as much

Figure 2. Potential energy surface of neutral [H_3,N,O]; zero-point corrected energies given in kcal mol^{-1} relative to H_2NOH (**2**)

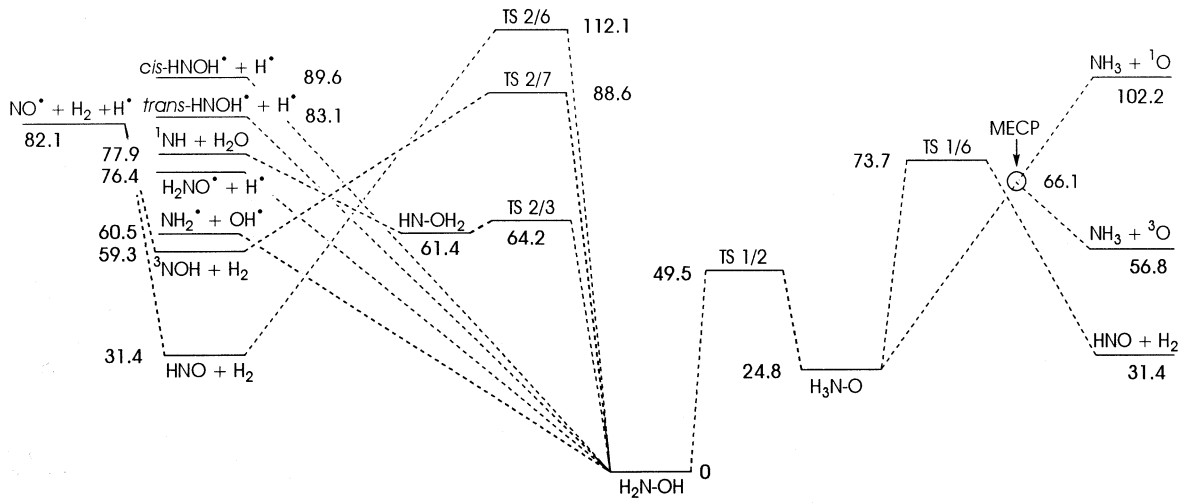

as 1.6 eV, although IE_a is comparable for both isomers.[8][9] A similar difference can be discerned for the recombination processes of an electron with the cations to the neutral molecules. In fact, these pronounced differences in physical properties may enable an experimental distinction of these two isomers.

The stability of the third neutral isomer, the imine-water complex **3**, has very much decreased compared to the cationic surface. The minimum structure is hardly more stable than the transition state of the [1,2]-H shift **TS 2/3**, and a further internal energy of 16.5 kcal mol^{-1} is sufficient to dissociate the molecule into ^{1}NH and H_2O. Dissociation into ^{3}NH and H_2O is exothermic by 25.5 kcal mol^{-1}, but a spin-forbidden process for **^{1}3**.

The relative heights of the exit channels are also different from the cationic surface, especially as far as the structure-indicative channels involving N−O bond cleavage are concerned. In this respect, dissociation of [H_3,N,O] into $H_2N^\bullet$ and $OH^\bullet$ represents the lowest lying, barrier-free exit channel with a relative energy of 60.5 kcal mol^{-1}, whereas the spin-allowed dissociation into O (^1D) and NH_3 becomes quite unfavorable with a relative energy of 102.2 kcal mol^{-1}. Therefore, the dissociation behaviour of the neutral isomers is expected to be quite different from that of the cations, in that for [H_3,N,O] formation of $H_2N^\bullet$ and $OH^\bullet$ should be more pronounced than NH_2^+ + $OH^\bullet$ for [H_3,N,O]$^{\bullet+}$. The relative stability of the closed-shell pair HNO + H_2 (31.4 kcal mol^{-1}) is much higher than $H^\bullet$ losses to yield the open-shell pairs $H_2NO^\bullet$ + $H^\bullet$ (76.4 kcal mol^{-1}), *trans*-HNOH$^\bullet$ + $H^\bullet$ (83.1 kcal mol^{-1}) and *cis*-HNOH$^\bullet$ + $H^\bullet$ (89.6 kcal mol^{-1}). However, HNO + H_2 formation is again hampered by significant activation barriers of 73.7 kcal mol^{-1} for 1,1-elimination from H_3NO and of 112.1 kcal mol^{-1} for 1,2-elimination from H_2NOH. Besides, NOH (^{3}A′′) and H_2 (E_{rel} = 59.3 kcal mol^{-1}) are obtained by 1,1-elimination of H_2 from H_2NOH, which is associated with a barrier of 88.6 kcal mol^{-1}.

Figure 3. Calculated bond lengths in pm and angles in degrees of relevant cationic [H_3,N,O]$^{\bullet+}$ species; for geometries of [H_2,N,O]$^+$ species pertinent to the present work, see ref.[6]

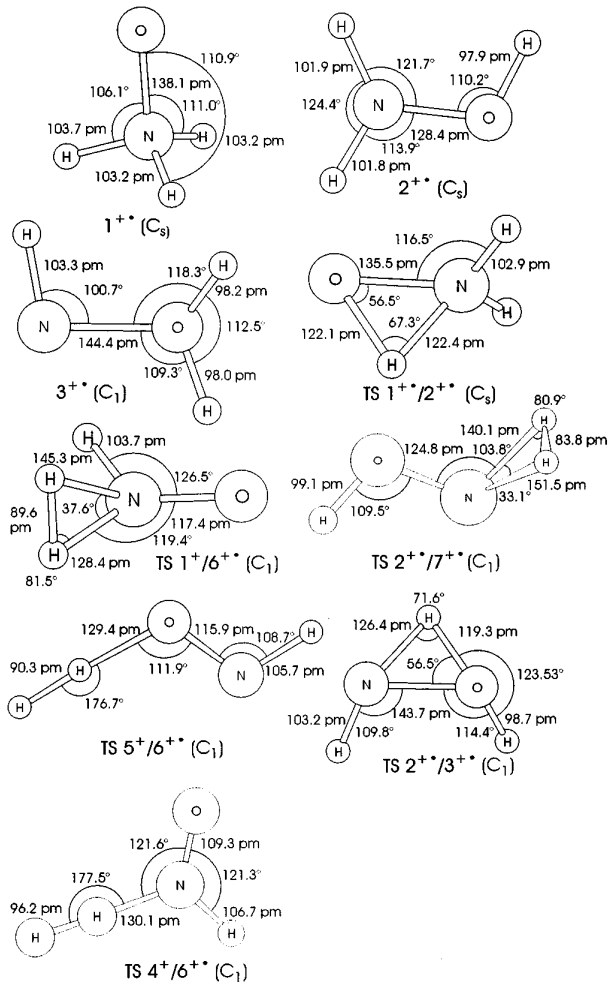

Figure 4. Calculated bond lengths in pm and angles in degrees of relevant neutral $[H_3,N,O]$ species

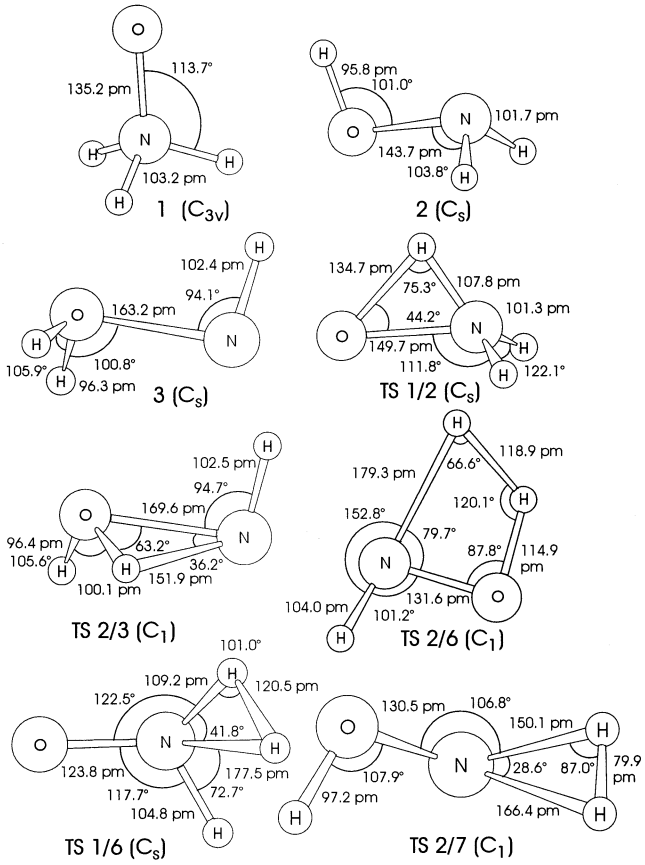

The NH_3 + O (^3P) exit channel has a comparatively low relative energy of 56.8 kcal mol^{-1}, but cannot be entered from the singlet surface in a spin-allowed manner. However, two processes that eventually yield ^3O + NH_3 should be mentioned briefly: (i) The dissociation of ^3H_3NO (^{3}**1**), which has an energy of 56 kcal mol^{-1} relative to **2** and 31.2 kcal mol^{-1} relative to $^1NH_3O$ (^{1}**1**), is spin-allowed. However, the N−O distance in geometry-optimized ^{3}**1** is 296 pm, revealing that the structure actually corresponds to a $^3O\cdots NH_3$ van der Waals complex with a binding energy of only 0.8 kcal mol^{-1}. A triplet structure for H_2NOH could not be located, but a second minimum on the triplet surface corresponding to $H_2N^{\bullet}\cdots H-O^{\bullet}$ with r_{N-H} = 200 pm was found with an energy of 58.7 kcal mol^{-1} relative to ^{1}**2**, only 1.9 kcal mol^{-1} below the separated species $H_2N^{\bullet}$ and $HO^{\bullet}$. (ii) In addition, the NH_3 + O (^3P) exit channel might be accessed by spin crossing of ^{1}**1** en route to oxygen dissociation. The highest spin crossing probability is achieved at geometries where both spin states possess the same energy. Therefore, the minimum energy crossing point (MECP) for the H_3N-O dissociation was located with a recently developed method.[10] Most efficient crossing is expected at N−O distances of 192 pm, where the molecule has an energy of 66.1 kcal mol^{-1} relative to **1**.

As far as $[H_3,N,O]^{\bullet-}$ anions are concerned, three minimum structures could be located that all correspond to weakly bound ion-dipole complexes.[4][11] The respective relative energies are E_{rel} = 0 for $HNH^{\bullet}\cdots OH^-$, E_{rel} = 3.1 kcal mol^{-1} for $HOH\cdots NH^{\bullet-}$ and E_{rel} = 7.7 kcal mol^{-1} for $H_2NH\cdots O^{\bullet-}$. None of the complexes possesses an intact N−O bond, and dissociations into $H_2N^{\bullet}$ and OH^- (E_{rel} = 15.3 kcal mol^{-1}), NH_3 and $O^{\bullet-}$ (E_{rel} = 23.3 kcal mol^{-1}) or into $HN^{\bullet-}$ and H_2O (E_{rel} = 27.3 kcal mol^{-1}) can occur easily. We would like to point out that both neutral isomers **1** and **2** possess negative vertical electron affinities, i.e. EA_v = −22.8 kcal mol^{-1} for **1** and EA_v = −47.4 kcal mol^{-1} for **2**. Thus, theory strongly suggests that a distinction of neutral **1** and **2** by electron attachment experiments, which have been applied successfully to the generation and identification of the neutral singlet water oxide molecule,[4][11] is not feasible for the $[H_3,N,O]$ system.

In conclusion, the quantum chemical calculations predict the existence of three $[H_3,N,O]^{\bullet+/0}$ isomers. Whereas the shapes of the neutral and cationic PES are similar concerning the hydroxylamine/ammonia oxide tautomerism, distinct differences exist with respect to the energetics of the fragmentation channels.

Experimental Results

The analysis of the hydroxylamine/ammonia oxide system based on dissociation products is hampered by an analytical problem, because the structure-indicative cleavages of the N−O bonds lead to fragments of equal masses, i.e. $NH_2^{\bullet}$ and O (both 16 amu) as well as NH_3 and $OH^{\bullet}$ (both 17 amu). Therefore, we decided to carry out additional experiments with the fully deuterated analogs $[D_3,N,O]$, such that the combination of the two sets of data allows for a deconvolution of the overlapping fragments, i.e. ND_2 and OD (both 18 amu) as well as ND_3 and D_2O (both 20 amu). In order to produce the three different isomers $\mathbf{1}^{\bullet+}$, $\mathbf{2}^{\bullet+}$, and $\mathbf{3}^{\bullet+}$, the following precursors were chosen. (i) A mixture of NH_3 and N_2O was subjected to chemical ionization in which one may envision N_2O as a donor for atomic oxygen to afford ammonia oxide cation $\mathbf{1}^{\bullet+}$. (ii) Pure hydroxylamine was ionized to (predominantly) yield $\mathbf{2}^{\bullet+}$. (iii) Surprisingly, electron ionization of an aqueous N_3H solution also yields reasonable amounts of $[H_3,N,O]^{\bullet+}$, and high mass-resolution and labeling experiments assured that the selected beam actually had the desired elemental composition. The mechanism of $[H_3,N,O]^{\bullet+}$ formation could not be established and seems particularly obscure for N_3H/H_2O. Although we cannot exclude rigorously ion-molecule reactions, the fact that the highest yields of $[H_3,N,O]^{\bullet+}$ are obtained under electron ionization conditions suggests that a volatile, hitherto uncharacterized N,H,O compound is liberated from an aqueous mixture of NaN_3 and H_2SO_4. Methods (i) and (iii) gave similar spectra (Table 3), but the $[H_3,N,O]^{\bullet+}$ intensities obtained from N_3H/H_2O were much higher than those from NH_3/N_2O. Thus, in the following discussion, the fragmentation patterns obtained for ionized

NH_2OH are compared with those for N_3H/H_2O and their deuterated analogues.

Table 3. Relative intensities of fragments generated from different $[H_3,N,O]$ and $[D_3,N,O]$ precursors

$[H_3,N,O]$ Experiment	Precursors	Fragment mass in amu 33	32	31	30	19	18	17	16	15	14
MI	NH_2OH		100	20	2			0.4	0.5		
	NH_3/N_2O		100	5				2			
	HN_3/H_2O		100	6	1			4			
CA	NH_2OH		100	18	27	0.4	1	3	4	0.6	0.2
	NH_3/N_2O		100	12	16	0.4	1	5	3	1	0.2
	HN_3/H_2O		100	14	19	1	2	11	4	1	0.2
NR	NH_2OH	100	71	12	20		1	11	16	3	1
	NH_3/N_2O	100	48	14	17			15	19	1	
	HN_3/H_2O	100	62	16	21	1	2	17	22	7	2
NR-CA	NH_2OH		100	24	38		2	9	13	2	2
	HN_3/H_2O		100	30	40			30	20		

$[D_3,N,O]$ Experiment	Precursors	Fragment mass in amu 36	34	32	30	22	20	18	16	14
MI	ND_2OD		100	2	1		0.5	0.6		
	ND_3/N_2O		100				4			
	DN_3/D_2O		100	1			12			
CA	ND_2OD		100	15	18	1	7	10	1	0.5
	ND_3/N_2O		100	10	13	1	14	9	2	1
	DN_3/D_2O		100	15	14	1	15	8	1	0.2
NR	ND_2OD	100	56	9	10		7	27	5	1
	ND_3/N_2O	100	31	5	10		6	15	2	
	DN_3/D_2O	100	56	17	18		15	51	17	2
NR-CA	ND_2OD		100	26	34		18	25	4	

The intensities of the metastable ion (MI) spectra are low, consistent with the fact that $[H_3,N,O]$ has only few degrees of freedom for the storage of internal energy. In all spectra, the by far dominant process corresponds to $H^\bullet$ loss to yield $[H_2,N,O]^+$, which is the lowest lying barrier-free exit channel of the system. However, as already mentioned neither this nor the other hydrogen loss channels are indicative as far as structural aspects are concerned. Thus, the following discussion is primarily based on the structurally indicative signals due to N−O bond cleavage. Unimolecular dissociation of ionized hydroxylamine yields fragments of masses 16 and 17 in a 1.3:1 ratio, while only mass 17 is observed in the MI experiment using the HN_3/H_2O mixture as precursor. Accordingly, the MI spectrum of $[D_3,N,O]^{\bullet+}$ obtained from DN_3/D_2O gives rise to a single signal at mass 20, which demonstrates that exclusively $ND_3^{\bullet+}$ is formed. In comparison, the MI spectrum of $ND_2OD^{\bullet+}$ is featured by two peaks at $m = 18$ and $m = 20$ in a 1.2:1 ratio, indicating that ND_2^+ as well as $ND_3^{\bullet+}$ are produced with ND_2^+ slightly dominating. Further, the combined analysis of the results obtained for the unlabeled and the labeled ions suggests that contributions of oxygen-containing fragments are minor in the MI mass spectra. This is consistent with the order of the *IE*s of the complementary fragments arising from $[H_3,N,O]$, i.e. $IE(NH_2) = 11.4$ eV vs. $IE(OH) = 13.0$ eV and $IE(NH_3) = 10.2$ eV vs. $IE(O) = 13.6$ eV.[5]

An increase of the internal energy of the molecules by collisional activation leads to much more abundant fragmentations. In addition, a fraction of "hot" molecules possesses lifetimes long enough to allow for extensive rearrangements preceding decomposition, which is indicated by fragments like $H_2O^{\bullet+}$ and H_3O^+ (or $D_2O^{\bullet+}$ and D_3O^+, respectively). Nonetheless, collisional activation with ions having keV energies promotes characteristic direct bond cleavages which are valuable for a structural characterization.

Due to collision-induced isomerization, the differences in the CA spectra of the two precursors are less pronounced compared to the metastable ion decay patterns. However, whereas ionized hydroxylamine shows an *m*/*z* 16/17 ratio of 1.3:1, this ratio amounts to 1:2.7 for the ion observed from the HN_3/H_2O mixture (Figures 5a and 5b). Analogous results are obtained with the deuterated compounds, in that the 18/20 ratio for ND_2OD is 1.4:1, as compared to 1:1.9 for the DN_3/D_2O mixture. In order to probe whether an alteration of the ion internal energy has any effect, CA spectra of $\mathbf{2}^{\bullet+}$ were also recorded at various ionization energies ranging from 10 to 100 V under EI conditions; in addition, **2** was ionized under CI conditions at higher source pressures. Except for the $HNO^{\bullet+}/NO^+$ ratio (see below), both variations, however, did not lead to significant changes of fragmentation patterns, suggesting that internal energy effects can be neglected to a first approximation.

The differences in the MI and CA spectra of the two precursors prove that the ion beam produced via HN_3/H_2O cannot consist of $\mathbf{2}^{\bullet+}$ alone. In fact, the absence of the signal at 16 amu in the MI spectra suggests that rather a pure beam of ammonia oxide ($\mathbf{1}^{\bullet+}$) is produced. The dominant

Figure 5. Mass spectra of $[H_3,N,O]^{\bullet+}$ ions generated from HN_3/H_2O and NH_2OH, respectively, as neutral precursors; CA spectra for HN_3/H_2O (a) and NH_2OH (b), $^+NR^+$ spectra for HN_3/H_2O (c) and NH_2OH (d), and $^+NR^+$/CA spectra for HN_3/H_2O (e) and NH_2OH (f)

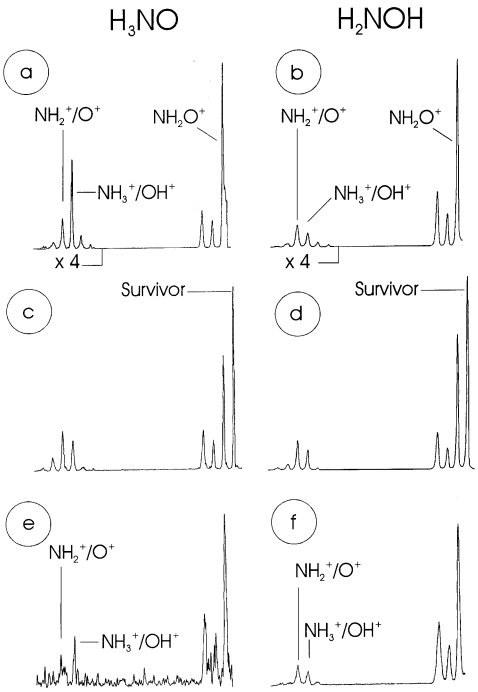

signal corresponds to $NH_3^{\bullet+}$, which is in line with an NH_3-O connectivity, whereas the dominant fragment of the NH_2OH precursor is NH_2^+, as expected for the NH_2-OH connectivity. In both MI and CA experiments, the HN_3/H_2O couple gives rise to a much more distinct and characteristic 16/17 ratio compared to NH_2OH. An explanation can be derived from the cationic potential energy surface. The $NH_3^{\bullet+}$ + O (^3P) exit channel is much lower in energy compared to NH_2^+ + $OH^\bullet$ (58 kcal mol^{-1} vs. 104 kcal mol^{-1}). Starting from $\mathbf{2}^{\bullet+}$, two decomposition paths compete. Compared to the direct bond cleavage to yield NH_2^+ + OH, the $NH_3^{\bullet+}$ + O exit channel is energetically favored, but entropically severely disfavored due to the necessity of a hydrogen migration. Especially in the MI experiment, the ions can store only a relatively low amount of internal energy; therefore, a fraction of molecules does not possess enough energy to access direct bond cleavage, but undergoes isomerization instead. Another indication for the formation of $\mathbf{1}^{\bullet+}$ from HN_3/H_2O is the fact that the intensity of the N−O cleavage relative to the base peak is much smaller for NH_2OH compared to HN_3/N_2O. A common feature of the CA spectra of both precursors is that NO^+ formation is more pronounced than $[H,N,O]^{\bullet+}$ formation, although the $NO^+/H_2/H^\bullet$ exit channel is 18.6 kcal mol^{-1} higher in energy than $HNO^{\bullet+}/H_2$ and 3.8 kcal mol^{-1} higher than $NOH^{\bullet+}/H_2$. The theoretical results show that for $[H,N,O]^{\bullet+}$ production, barriers of 89.5 kcal mol^{-1} for 1,1-elimination from $\mathbf{1}^{\bullet+}$ and of 92.3 kcal mol^{-1} for 1,1-elimination from $\mathbf{2}^{\bullet+}$ have to be overcome. Therefore, *every* generated $[H,N,O]^{\bullet+}$ + H_2 unit has an internal excess energy of at least 19.1 kcal mol^{-1}. This excess energy is sufficient to convert a considerable fraction of $[H,N,O]^{\bullet+}$ immediately to NO^+ and $H^\bullet$. It was found that the $NO^+/[H,N,O]^{\bullet+}$ ratio varies easily with experimental conditions, pointing to a high sensitivity of this particular ratio towards the internal energy. Unimolecular decomposition of both precursors yields, next to dominant $H^\bullet$ loss, small amounts of $[H,N,O]^{\bullet+}$ and NO^+, the $[H,N,O]^{\bullet+}$ signal being higher in each case. In contrast to that, unimolecular decomposition of $\mathbf{4}^+$ and $\mathbf{5}^+$ produces mainly NO^+ and only minor amounts of $HNO^{\bullet+}$ cation.[6] Therefore, it can be concluded that at least in the low-energy regime, $[H,N,O]^{\bullet+}$ and NO^+ fragments in $[H_3,N,O]^{\bullet+}$ are not generated via $[H_2,N,O]^+$ as an intermediate, but produced on a different way, probably by H_2 elimination; this conjecture is completely in line with the theoretical predictions. Finally, it should be noted that signals due to H_3O^+ ions are minor in CA spectra and not observed at all in MI spectra of both precursors, although fragmentation into H_3O^+ and N (^4S) is predicted to be the thermodynamically most favorable exit channel of $[H_3,N,O]^{\bullet+}$. Obviously, access to this fragmentation is severely hampered by the kinetic restrictions associated with extensive isomerization and spin crossing.

After having shown that two different cationic $[H_3,N,O]^{\bullet+}$ precursors can be distinguished, an experimental differentiation of the corresponding neutral counterparts **1** and **2** is attempted. One approach to neutral ammonia oxide is based on the strategy shown in Scheme 1. Thus, a precursor molecule H_2N-OR is protonated with a suitable CI gas. If the preferred protonation site is nitrogen, and if the group R can form a stable cation, metastable ion decay of H_3N^+-O-R may lead to R^+ and neutral ammonia oxide (H_3NO). This route can be followed by performing CIDI (collision induced dissociative ionization) experiments in which after deflection of all charged species from the beam, the neutrals are subsequently reionized and detected.[12] CIDI experiments were performed with $H_2NOSiMe_3$ (**9**), $H_2NOSiMe_2Ph$, and $H_2NOSi\mathit{t}BuPh_2$ as precursors.[13] Although the stabilities of the cationic leaving groups should increase in the order $SiMe_3^+$ < $SiMe_2Ph^+$ < $Si\mathit{t}BuPh_2^+$, meaningful CIDI spectra could only be obtained for **9**. This is probably a consequence of the fact that the effective kinetic energies of the neutral $[H_3,N,O]$ fragments decrease with increasing size of the precursor, which lowers the reionization yields of $[H_3,N,O]$. The MI spectrum of $H_3NOSiMe_3^+$, which was generated by protonation of **9** with methane as CI gas,[14] is featured by losses of 15 amu (30%), 16 amu (100%), and 33 amu (50%), demonstrating that the heaviest neutral fragment lost is actually $[H_3,N,O]$. The most important feature of the CIDI spectrum is that reionized neutral $[H_3,N,O]$ constitutes the base peak in the spectrum. According to the MI spectrum, no peaks with masses higher than 33 should be present in a pure CIDI spectrum. Small signals between 40 and 47 amu indicate, however, that few NR processes occur due to diffusion of the reionization gas through the deflector region of the mass spectrometer.[12] The key issue is, however,

whether the peak at *m*/*z* 33 can be assigned unambiguously to reionized ammonia oxide. Mainly two concerns discard the CIDI experiment as a proof. Although theory predicts that *N*-protonation of **9** is favored over *O*-protonation by 16 kcal mol^{-1}, it cannot be excluded that a fraction of molecules is protonated at the oxygen atom, because the protonation with methane as CI gas is strongly exothermic at either side, i. e. 86.4 kcal mol^{-1} and 70.4 kcal mol^{-1}, respectively.[15] Thus, one might argue that the observed reionized $[H_3,N,O]$ stems from the *O*-protonated species, which produces hydroxylamine concomitantly with the generation of $SiMe_3^+$. Moreover, even if exclusive initial *N*-protonation is assumed, one cannot rule out a possible [1,2]-H shift from the nitrogen to the oxygen atom prior to or concerted with $SiMe_3^+$ loss. Both objectives would be disprovable if it was possible to examine *N*-protonated $Me_3SiNHOH$, but this compound has not been synthesized yet. Due to the concerns mentioned, for the time being the CIDI experiments should be regarded as an experimental hint for neutral ammonia oxide rather than a proof.

Scheme 1

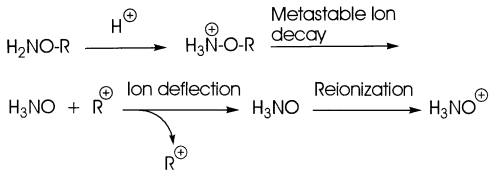

In a different approach to generate the neutral $[H_3,N,O]$ molecule, the cationic beam was neutralized with xenon, and after removal of all ionic species from the beam, the neutrals were reionized with oxygen, subsequently mass-analyzed and detected.[3] The base peak of all neutralization-reionization spectra belongs to intact $[H_3,N,O]$, which demonstrates the distinct stability of neutral $[H_3,N,O]$ (Figures 5c and 5d). As low-mass fragments represent a superposition of decompositions of the projectile ion, the neutral transient, and the reionized species, structural information of the neutrals is difficult to achieve from fragment ion analysis. However, we note that the most intense peak in the lower mass region corresponds to $NH_2^\bullet$ ($ND_2^\bullet$) for both precursors, in line with the theoretical predictions for this exit channel.

The mere observation of an NR survivor ion arising from cationic ammonia oxide does, however, not prove the existence of neutral ammonia oxide, as the structural integrity might have been lost by isomerization at the neutral stage. Therefore, the structure of reionized $[H_3,N,O]$ survivor ions was examined by a collisional activation experiment (Figures 5e and 5f). For H_2NOH and its deuterated analog, CA and NR/CA spectra are practically indistinguishable, which proves that no significant isomerization occurs at the neutral stage. The corresponding NR/CA experiment with the ammonia oxide precursor was conducted close to the detection limit of the instrument. Although the signal-to-noise ratio is poor, it can be seen that the fragmentation pattern in the structurally indicative region again resembles the observed CA pattern for the ammonia oxide cation rather than that of ionized NH_2OH (Fig. 5e and 5f). Thus, at least a complete isomerization **1** → **2** at the neutral stage seems improbable. Further, the intense survivor ion in NR spectra indicates favorable Franck-Condon factors for single-electron reduction to neutral **1**, being in line with the fact that the geometries of neutral and cationic ammonia oxide are very similar. The $NH_2^+/NH_3^{\bullet+}$ ratio in the NR/CA spectrum of $\mathbf{2}^{\bullet+}$ (Figure 5f) also implies that hydroxylamine does not isomerize during the NR experiment, in spite of the much less favorable Franck-Condon overlap of cation and neutral.

In conclusion, relevant points of the cationic and neutral $[H_3,N,O]^{\bullet+/0}$ surface have been calculated on a high theoretical level, predicting the existence of three different $[H_3,N,O]$ isomers. Information obtained from the experiments, combined with the theoretical results, show that two cationic $[H_3,N,O]^{\bullet+}$ species can be distinguished in the gas phase. Furthermore, the experiments strongly suggest the existence of neutral ammonia oxide, although a definitive proof cannot be provided yet. This ambiguity is probably due to (i) the fact that the differences of the NR spectra of $\mathbf{1}^{\bullet+}$ and $\mathbf{2}^{\bullet+}$ are minor suggesting a compensation of Franck-Condon effects in conjunction with the different fragmentation channels accessible and (ii) the failure to perform $^-CR^+$ and/or $^-NR^+$ experiments as far as meaningful information about connectivity is concerned. Nonetheless, the NR/CA experiments presented here are very much in favor of the generation of $\mathbf{1}^{\bullet+}$ upon ionization of HN_3/H_2O as well as the generation of neutral ammonia oxide **1**.

We are grateful to the *Deutsche Forschungsgemeinschaft*, the *Fonds der Chemischen Industrie*, and the *Volkswagen-Stiftung* for financial support. M. B. and I. K. acknowledge the *Stiftung Stipendien-Fonds des Verbandes der Chemischen Industrie* for Ph. D. scholarships. We thank Dr. *J. N. Harvey* for helpful discussions concerning the quantum chemical calculations.

Experimental Section

The experiments were performed with a modified VG/ZAB/HF/AMD four-sector mass spectrometer of *BEBE* configuration (*B* stands for magnetic and *E* for electric sector), which has been described in detail elsewhere.[16] NH_2OH and N_3H/H_2O were ionized by a beam of electrons (100 eV) in an electron ionization source (repeller voltage ca. 30 V). NH_3/N_2O mixtures were ionized under chemical ionization conditions. The ions of interest were accelerated to 8 keV and mass-selected by means of *B*(1)/*E*(1) at a resolution of $m/\Delta m \geq 3000$; isobaric impurities, i.e. O_2H^+ and $N_2H_5^+$ for $[H_3,N,O]$ or $N_2D_4^{\bullet+}$ and $D_2O_2^{\bullet+}$ for $[D_3,N,O]$ were either absent or baseline-resolved. Unimolecular fragmentations occurring in the field-free region preceding the second magnet are referred to as metastable ion spectra. For collisional activation experiments, helium (80% transmission, T) was admitted to a collision cell located between *E*(1) and *B*(2). In these MI and CA experiments, the ionic fragments were recorded by scanning *B*(2). For comparison with the NR/CA spectra (see below), MI and CA experiments were also performed with *B*(1)/*E*(1)/*B*(2)-mass-selected ions, scanning products with *E*(2). For NR experiments, cations were neutralized

by collisions with xenon (80% T); unreacted ions were removed from the beam. Subsequent reionization of the neutrals was achieved by collision with oxygen (80% T), and the resulting cationic fragments were recorded by scanning *B*(2). For NR/CA experiments, the survivor ions of the NR experiment were mass-selected with *B*(2), collided with helium (80% T), and the produced fragments were recorded by scanning *E*(2). In order to improve the signal-to-noise ratio, 5−100 spectra were accumulated and online-processed with the AMD-Intectra data system.

ND_2OD was obtained by repeated recrystallization of pure NH_2OH in CH_3CH_2OD. Pure NH_2OH was deliberated from $NH_2OH \cdot HCl$ with NaOEt.[17] ND_3 was produced by deuterolysis of Mg_3N_2 with D_2O. Aqueous HN_3 was produced by dropping concentrated sulfuric acid into a solution of NaN_3 in water. The concentration of HN_3 solutions was about 1−5%. $H_2NOSiMe_3$, $H_2NOSiMe_2Ph$, and $H_2NOSitBuPh_2$ were synthesized by treating hydroxylamine with the corresponding chlorosilanes $ClSiR_3$ in dichloromethane.[18] All chemicals were introduced in the ion source via the metal-free teflon/glass inlet system.[19]

Ab initio quantum-mechanical calculations were performed with IBM RS/6000 workstations and Pentium PCs using Gaussian 94.[20] For trimethylsilyl-substituted species, geometries were fully optimized at the HF/6-31G* level, and single-point energies were calculated at the MP2/6-31G* level. For all other species, full geometry optimizations and frequency calculations were carried out at the MP2/6-311G(d,p) level. The effect of using larger basis sets and a better correlation treatment was examined by performing single-point MP2/6-311+G(3df,2p) and CCSD(T)/6-311G(d,p) calculations at the previously optimized geometries. These results were further used to determine extrapolated[21] CCSD(T)/6-311+G(3df,2p) energies in an approach similar to the well-known G2 method.[23] All data in Tables 1 and 2 include the unscaled MP2/6-311G** zero-point energy corrections. The relative energy of ^1O was determined by adding the experimental value for the $^3P \rightarrow {}^1D$ excitation (1.967 eV)[24] to the calculated total energy of ^3O. Analogously, the relative energy of ^2N was determined by adding the experimental value for the $^4S \rightarrow {}^2D$ excitation (2.383 eV)[24] to the calculated total energy of ^4N. The minimum energy crossing point (MECP) of H_3NO was located by employing a recently developed hybrid method[10] which calculates energy gradients at the MP2/6-311G(d,p) level and energies of stationary points at the CCSD(T)/6-311G(d,p) level. The geometries of both spin states were adjusted until the energy difference between them was smaller than 0.06 kcal mol^{-1}.

☆ Dedicated to Professor Dr. *Ernst Schmitz*, Berlin, on the occasion of his 70th birthday.

[1] [1a] B. Kallies, R. Mitzner, *J. Phys. Chem. B* **1997**, *101*, 2959. − [1b] T. P. Cunningham, D. L. Cooper, J. Gerrat, P. B. Karadakov, M. Raimondi, *Int. J. Quantum Chem.* **1996**, *60*, 393. − [1c] R. Ponec, M. Krack, K. Jug, *Theor. Chim. Acta* **1996**, *93*, 165. − [1d] N. N. Kharabaev, V. V. Rachkovskii, A. D. Garnovkii, *Zh. Obshch. Khim.* **1995**, *65*, 1650 (*Chem. Abstr.* **1996**, *125*, 151522x). − [1e] R. D. Bach, A. L. Owensby, C. Gonzales, H. B. Schlegel, J. J. W. McDouall, *J. Am. Chem. Soc.* **1991**, *113*, 6001. − [1f] S. M. Bachrach, *J. Org. Chem.* **1990**, *55*, 1016. − [1g] Y.-Z. Han, D.-Z. Zhu, C.-D. Zhao, *Chin. J. Chem.* **1990**, *5*, 405. − [1h] J. A. Pople, K. Raghavachari, M. J. Frisch, J. S. Binkley, P. v. R. Schleyer, *J. Am. Chem. Soc.* **1983**, *105*, 6389. − [1i] F. Grein, J. L. Lawlor, *Theor. Chim. Acta* **1983**, *63*, 161. − [1j] H. Wallmeier, W. Kutzelnigg, *J. Am. Chem. Soc.* **1979**, *101*, 2804. − [1k] C. Trindle, D. D. Shillady, *J. Am. Chem. Soc.* **1973**, *95*, 703.

[2] [2a] D. Luckhaus, *Ber. Bunsenges. Phys. Chem.* **1997**, *101*, 346. − [2b] B. Kuhn, O. V. Boyarkin, T. R. Rizzo, *Ber. Bunsenges. Phys.* **1997**, *101*, 339. − [2c] D. Luckhaus, *J. Chem. Phys.* **1997**, *106*, 8409. − [2d] M. N. Hughes, K. Shrimanker, *Inorg. Chim. Acta* **1976**, *18*, 69.

[3] [3a] C. A. Schalley, G. Hornung, D. Schröder, H. Schwarz, *J. Chem. Soc. Rev.* **1998**, *27*, 91. − [3b] N. Goldberg, H. Schwarz, *Acc. Chem. Res.* **1994**, *27*, 347. − [3c] F. Turecek, *Org. Mass Spectrom.* **1992**, *27*, 1087.

[4] Two problems closely related to $[H_3,N,O]$ concerning the $HOOH/H_2OO$ and the $HNNH/H_2NN$ tautomerism have been investigated by mass spectrometry: For $[H_2,O_2]$, see: D. Schröder, C. A. Schalley, N. Goldberg, J. Hrušák, H. Schwarz, *Chem. Eur. J.* **1996**, *2*, 1235; for $[H_2,N_2]$, see: N. Goldberg, M. C. Holthausen, J. Hrušák, W. Koch, H. Schwarz, *Chem. Ber.* **1993**, *126*, 2753.

[5] S. G. Lias, J. F. Liebmann, J. L. Holmes, R. D. Levin, W. G. Mallard, *J. Phys. Chem. Ref. Data* **1988**, *17*, 695.

[6] For a combined MS and theoretical study of $[H_2,N,O]^+$ ions, see: [6a] D. Schröder, F. Grandinetti, J. Hrušák, H. Schwarz, *J. Phys. Chem* **1992**, *96*, 4841. − [6b] F. Grandinetti, J. Hrušák, D. Schröder, H. Schwarz, *J. Phys. Chem.* **1992**, *96*, 2100. − [6c] C. Lifshitz, P. J. A. Ruttink, G. Schaftenaar, J. K. Terlouw, *Mass Spectrom. Rapid Commun.* **1987**, *1*, 61.

[7] Our calculated dipole moments agree fairly well with the experimentally determined values of 0.59 D for hydroxylamine (taken from *Selected Values of Electric Moments for Molecules in the Gas Phase*, U.S. Department of Commerce, National Bureau of Standards, **1967**) and of 5.0 D for Me_3NO (taken from: N. Hacket, R. J. W. Fevre, *J. Chem. Soc.* **1961**, 1612).

[8] The discrepancy between our calculated value for IE_a(**2**) = 9.15 eV and the literature values (9.6 eV[9a] and 10.0 eV[9b]) derived from photoelectron spectra is quite high. We ascribe it to the absence of the 0-0 transition in the experiment, yielding an overestimation of IE_a. The calculated value for IE_v(**2**) = 10.72 eV and the experimental values (10.6 eV[9a] and 10.56 eV[9b]) agree much better.

[9] [9a] I. A. Koppel, U. M. Mölder, R. J. Pikver, *Org. React.* **1983**, *20*, 45. − [9b] R. E. Kutina, G. L. Goodman, J. Berkowitz, *J. Chem. Phys.* **1982**, *77*, 1664.

[10] [10a] J. N. Harvey, M. Aschi, H. Schwarz, W. Koch, *Theor. Chem. Acc.* **1998**, *99*, 95. − [10b] D. Schröder, C. Heinemann, H. Schwarz, J. N. Harvey, S. Dua, S. J. Blanskby, J. H. Bowie, *Chem. Eur. J.*, in press.

[11] [11a] J. Hrušák, H. Friedrichs, H. Schwarz, H. Razafinjanahary, H. Chermette, *J. Phys. Chem.* **1996**, *100*, 100. − [11b] S. Humbel, I. Demachy, P. C. Hilberty, *Chem. Phys. Lett.* **1995**, *247*, 126.

[12] [12a] M. J. Polce, S. Beranova, M. J. Nold, C. Wesdemiotis, *J. Mass Spectrom.* **1996**, *31*, 1073. − [12b] J. L. Holmes, A. A. Mommers, *Org. Mass Spectrom.* **1984**, *19*, 460. − [12c] P. C. Burgers, J. L. Holmes, A. A. Mommers, J. E. Szulejko, J. K. Terlouw, *Org. Mass Spectrom.* **1984**, *19*, 442.

[13] Attempts to protonate $F_3CCONHOH$ and $H_2NOCOCF_3$ lead to loss of HF instead of the desired loss of neutral H_3NO.

[14] Whereas protonation with H_2 was not feasible, use of isobutane as CI gas gave the same results as with methane.

[15] The heats of reaction were determined by substracting the proton affinity of methane (132 kcal mol^{-1}) from the calculated proton affinity for *N*- and *O*-protonation of **9**. The calculated total energies including zero point corrections are −538.8831 hartree for $H_2NOSiMe_3$, −539.4069 hartree for $H_3NOSiMe_3^+$ and −539.2033 hartree for $H_2NOHSiMe_3^+$.

[16] [16a] C. A. Schalley, D. Schröder, H. Schwarz, *Int. J. Mass Spectrom. Ion Processes* **1996**, *153*, 173. − [16b] R. Srinivas, D. Sülzle, W. Koch, C. H. DePuy, H. Schwarz, *J. Am. Chem. Soc.* **1991**, *113*, 5970. − [16c] R. Srinivas, D. Sülzle, T. Weiske, H. Schwarz, *Int J. Mass Spectrom. Ion Processes* **1991**, *107*, 368.

[17] R. Steudel, P. W. Schenk in *Handbuch der präparativen anorganischen Chemie* (Ed.: G. Brauer), F. Enke Verlag, Stuttgart, **1975**, p. 464.

[18] J. C. Bottaro, C. D. Clifford, A. Dodge, *Synth. Commun.* **1985**, *15*, 1333.

[19] C. A. Schalley, R. Wesendrup, D. Schröder, T. Weiske, H, Schwarz, *J. Am. Chem. Soc.* **1995**, *117*, 7711.

[20] M. J. Frisch, G. W. Trucks, H. B. Schlegel, P. M. W. Gill, B. G. Johnson, M. A. Robb, J. R. Cheeseman, T. Keith, G. A. Petersson, J. A. Montgomery, K. Raghavachari, M. A. Al-Laham, V. G. Zakrzewski, J. V. Ortiz, J. B. Foresman, J. Cioslowski, B. B. Stefanov, A. Nanayakkara, M. Challacombe, C. Y. Peng, P. Y. Ayala, W. Chen, M. W. Wong, J. L. Andres, E. S. Replogle, R. Gomperts, R. L. Martin, D. J. Fox, J. S. Binkley, D. J. Defrees,

J. Baker, J. P. Stewart, M. Head-Gordon, C. Gonzalez, J. A. Pople, *Gaussian 94, Revision E.1*, Gaussian, Inc., Pittsburgh PA, **1995**.

[21] E[CCSD(T)/6-311+G(3df,2p)] $\approx$ E[CCSD(T)/6-311G(d,p)] + E[MP2/6-311+G(3df,2p)] − E[MP2/6-311G(d,p)] + ZPVE; for details, see ref.[22].

[22] [22a] C. W. Bauschlicher, H. Partridge, *J. Chem. Phys.* **1995**, *103*, 1788. − [22b] L. A. Curtiss, K. Raghavachari, P. C. Redfern, J. A. Pople, *J. Chem. Phys.* **1997**, *106*, 1063.

[23] L. A. Curtiss, K. Raghavachari, G. W. Trucks, J. A. Pople, *J. Chem. Phys.* **1991**, *94*, 7221.

[24] G. Herzberg, *Molecular Spectra and Molecular Structure*, vol. 1, 2nd ed., Krieger Publishing Company, Malabar, **1993**, p. 447.

[98147]